

Deconvolution of Charge Injection Steps in Quantum Yield Multiplication on Silicon

H. J. Lewerenz and J. Stumper

Bereich Strahlenchemie, Hahn Meitner Institut, Glienicke Strasse 100, 1000 Berlin 39, Federal Republic of Germany

L. M. Peter

Department of Chemistry, The University, Southampton SO9 5NH, United Kingdom

(Received 6 July 1988)

An unusual photocurrent multiplication effect at the *n*-silicon/electrolyte interface which gives rise to quantum efficiencies approaching 400% has been investigated by intensity-modulated photocurrent spectroscopy. This technique has shown that the process involves hole capture followed by the successive injection of three electrons by surface intermediates. Kinetic analysis of this effect shows that the rate constants for electron injection are unusually low at between 1 and 10^3 s^{-1} .

PACS numbers: 73.40.Mr, 82.20.Pm, 82.45.+z, 82.50.Cr

Anomalously high quantum yields ($Q=2$) during semiconductor photodissolution were first observed at the germanium-electrolyte interface.¹ The phenomenon is referred to as current doubling since it corresponds to the transfer of two electrons per absorbed photon. In recent years, an analogous effect on Si has been observed,²⁻⁵ and even quadrupling of the photocurrent ($Q=4$) has been reported.⁴ This remarkable effect has been explained tentatively by the assumption that light-induced surface complexes located energetically at or above the conduction band are able to inject electrons into the silicon. Up to now, no decisive experimental proof of such a mechanism has been available, although a surface analytical investigation of photocurrent doubling has been performed recently.⁶ We present here for the first time experimental proof that the quantum-yield-multiplication effect is due to hole capture followed by the relatively slow injection of three electrons by surface intermediates.

The intensity-modulated photocurrent technique⁷⁻⁹ was chosen for the investigation on account of its unique capabilities for the determination of rate constants for photoinduced charge transfer. The principle of the method is shown in Fig. 1. The optoacoustic modulator

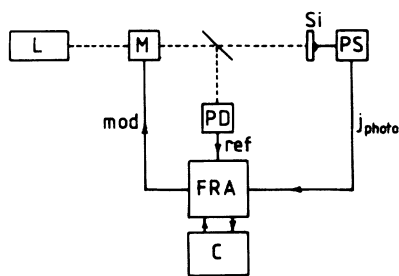


FIG. 1. Experimental arrangement. C is the microcomputer, FRA the frequency-response analyzer, L the laser, M the optoacoustic modulator, PD the photodiode, PS the potentiostat, and Si is the silicon electrode in contact with electrolyte.

produces a sinusoidal intensity modulation of the laser beam incident on the electrode, and a reference signal is provided by the photodiode which samples the incident beam. The magnitude and phase of the photocurrent are compared with those of the incident light by the frequency-response analyzer. The potential of the Si electrode is controlled by a high-bandwidth potentiostat.

Under suitably chosen experimental conditions, *n*-Si exhibits photocurrent multiplication in aqueous ammonium fluoride solutions.¹⁰ The photocurrent j_{photo} is then due to superimposition of the hole flux j_p into the surface and the electron flux j_n injected by surface intermediates;

$$j_{\text{photo}} = j_p + j_n. \quad (1)$$

It is not possible to separate j_p and j_n by conventional dc photocurrent techniques, but the photocurrent response to periodic or transient illumination allows them to be deconvoluted since the time scales associated with hole capture and electron injection will generally not be the same. If there is a time delay associated with electron injection, the phase and amplitude of the photocurrent

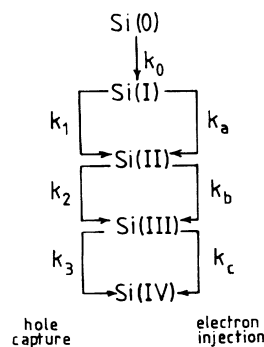


FIG. 2. Kinetic scheme for the photodissolution of *n*-Si showing the competition between hole capture (k_1 , k_2 , and k_3) and electron injection (k_a , k_b , and k_c).

will depend on the modulation frequency of the incident light, and the rate constants for the electron-transfer steps contributing to j_n can then be obtained.

Photodissolution of n -Si involves competition between hole capture and electron injection as illustrated schematically in Fig. 2. This reaction scheme leads to a set of linear differential equations that is readily solved for the steady state.¹⁰ In the low-intensity limit where electron injection predominates, Q will approach 4, whereas at higher intensities it will fall, eventually reaching 1 when electron injection can no longer compete with hole capture. This is in accord with reported experimental data,⁴ but no absolute values of the rate constants can be deduced from these measurements. By contrast, frequency-domain analysis provides kinetic information directly. For the case where all hole-capture steps except the first can be neglected (low-intensity limit), Eq. (1) can be written as

$$j_{\text{photo}} = j_p + k_a C(\text{I}) + k_b C(\text{II}) + k_c C(\text{III}), \quad (2)$$

where k_a , k_b , and k_c are first-order rate constants for electron injection and $C(\text{I})$, $C(\text{II})$, and $C(\text{III})$ are the surface concentrations of the injecting intermediates Si(I), Si(II), and Si(III).

Each electron-injection step gives rise to a characteristic time constant equal to the reciprocal of the corresponding first-order rate constant. This is illustrated by Fig. 3, which shows complex-plane plots of the quantum

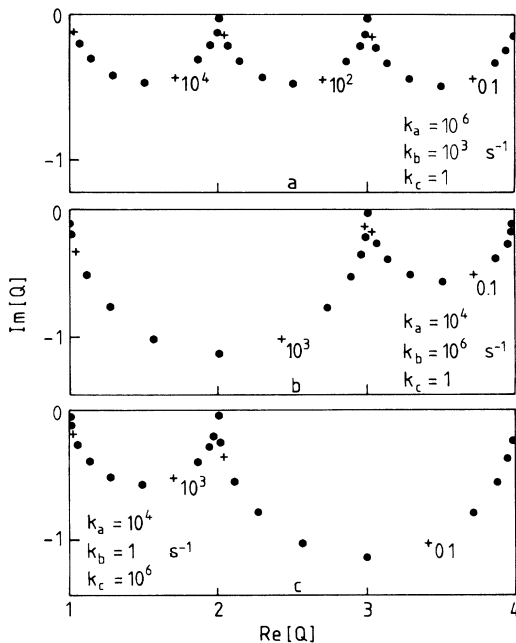


FIG. 3. Theoretical modulated photocurrent responses showing the time constants associated with electron injection. The rate constants (s^{-1}) for electron injection are shown in the figures.

efficiency

$$\hat{Q} = \hat{j}_{\text{photo}} / \hat{j}_p = \text{Re}(Q) + i \text{Im}(Q), \quad (3)$$

calculated for three sets of rate constants k_a , k_b , and k_c . The limiting values of Q are 4 (zero-frequency intercept) and 1 (high-frequency intercept), and the values of the rate constants can be obtained from the frequencies corresponding to the minima of the semicircles. The complete theoretical development¹⁰ includes the effects of recombination and of the RC time constant of the cell, but these effects are negligible under the experimental conditions used in this study.

Experiments were carried out on $\langle 111 \rangle$ n -Si wafers ($N_d = 4 \times 10^{15} \text{ cm}^{-3}$) in 6.5M ammonium fluoride solutions at pH 5.4 and in potassium phthalate buffer at pH 4.4. Measurements were made at 442 nm (He-Cd laser) and 632.8 nm (He-Ne laser), and the incident photon flux was calibrated with a silicon photodiode immersed in the solution and corrected for reflection losses. Solutions were prepared from AnalaR reagents with ultra-pure water and purged with oxygen-free nitrogen.

The existence of a photocurrent quadrupling effect in the fluoride solution was verified initially by steady-state measurements at low photon fluxes ($< 10^{13} \text{ cm}^{-2} \text{ s}^{-1}$). After correction for reflection losses, the maximum quantum yield in the saturation photocurrent region was found to be 3.6 ± 0.2 . By comparison, the quantum yield measured in the phthalate buffer solution was close to unity.

Intensity-modulated photocurrents were measured with 80% modulation depth in the frequency range 10 mHz to 65 kHz, and the response observed in fluoride solution is shown in Fig. 4. Measurements were also made with phthalate buffer, and the photocurrent in this case was found to be independent of frequency with $Q=1$. In the absence of electron injection, the photocurrent is due entirely to rapid capture of photogenerated holes, and there is negligible phase difference between excitation and photocurrent.

The shape of the complex-plane plot for n -Si in ammonium fluoride resembles the theoretical response

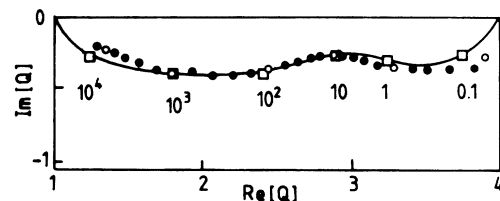
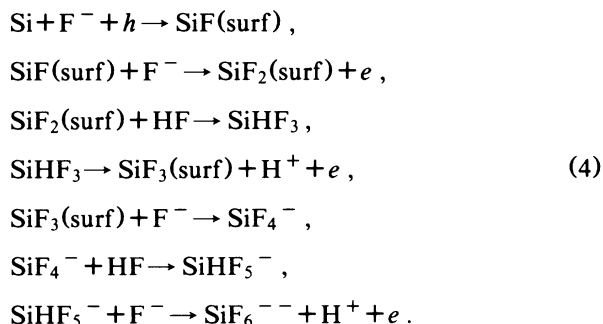


FIG. 4. Experimental modulated photocurrent response (circles) observed with $\langle 111 \rangle$ Si in 6.5M NH_4F solution (pH 5.4) at 1.5 V vs saturated calomel reference electrode (filled circles). The line and squares show the theoretical response calculated for $k_a = 2 \times 10^4 \text{ s}^{-1}$, $k_b = 500 \text{ s}^{-1}$, $k_c = 0.5 \text{ s}^{-1}$, and a standard deviation of $1.5 kT$ in activation energy for electron injection.

shown in Fig. 3(b), although the experimental semicircles are flattened as the result of surface inhomogeneity (see below). The first two electron-injection steps cannot be deconvoluted from the response, which shows that k_b is either of the same order of magnitude as k_a or possibly larger. The injection of the third electron is about 3 orders of magnitude slower, giving rise to the second semicircle at frequencies below 10 Hz.

Since there is evidence for mixed coverage with -H, -F, and possibly -OH ligands,^{6,11} we propose the following scheme which includes surface hydrogenated species:



Evidence for the involvement of SiHF_3 in the reaction scheme has been obtained by Fourier-transform infrared measurements.¹² The last electron-injection step is associated with the rupture of the final Si-Si bond and the formation of SiF_6^{--} in a three-step reaction which is likely to occur on a longer timescale than the earlier two steps.

The flattening of the semicircles evident in Fig. 4 has also been observed in the case of current doubling at *p*-GaAs.⁹ It can be modeled by the assumption of a normal distribution of activation energies (E_a) for the electron-injection steps associated with different dissolu-

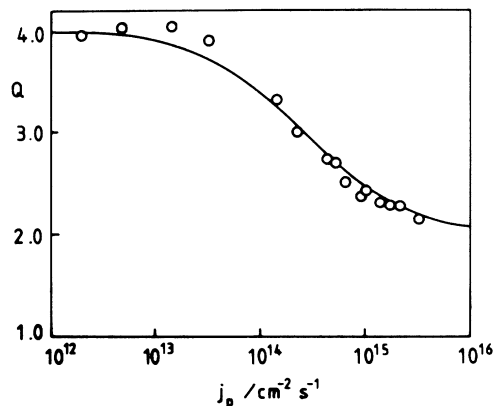


FIG. 5. Comparison of the experimental intensity dependence of the steady-state photocurrent quantum efficiency in fluoride solution reported in Ref. 4 (open circles) with the results of calculations based on the kinetic scheme shown in Fig. 2. The hole-capture cross sections are $\sigma_1 = 10^{-13} \text{ cm}^{-2}$, $\sigma_2 = \sigma_3 = 3 \times 10^{-20} \text{ cm}^{-2}$.

tion sites on the $\langle 111 \rangle$ surface.¹⁰

The rate constants k_a , k_b , and k_c can be expressed in the form

$$k = \nu \exp(-E_a/kT), \tag{5}$$

where E_a is an activation energy and ν is a preexponential factor. If ν is assumed to be of the order of 10^{12} s^{-1} , the activation energy for the final bond-breaking step is 0.65 eV. This value can be compared with the bond energies for Si-H and Si-F in SiH_4 and SiF_4 , which are, respectively, 3.38 and 5.88 eV, and with the Si-Si bond energy in the solid, which is of the order of 1 eV.

The values of k_a , k_b , and k_c were substituted into the steady-state solution for the general reaction scheme and the rate constants for hole capture by the intermediates Si(I), Si(II), and Si(III) were then varied to give the best fit to the experimental intensity dependence of the quantum efficiency.⁴ The results are shown in Fig. 5. The second-order rate constants for hole capture can be written in the form

$$k = \sigma_p v_p / \delta \approx 3 \sigma_p \times 10^{13} \text{ cm}^2 \text{ s}^{-1}, \tag{6}$$

where σ_p is the capture cross section for holes, v_p is the thermal velocity of holes, and δ is a reaction length of the order of an atomic diameter. The cross section for hole capture by the first intermediate Si(I) is therefore of the order of 10^{-13} cm^2 , whereas the cross sections for hole capture by the next two intermediates, Si(II) and Si(III) appear to be smaller by a factor of more than 10^6 . It follows that successful hole capture by intermediate Si(II) and Si(III) involves energies of activation of around 0.3 to 0.4 eV. Hole capture by Si(I), on the other hand, is evidently associated with a much smaller activation energy. These observations can be rationalized in terms of thermally activated bond rupture in the reaction scheme of Fig. 2, although contributions from Coulombic terms and solvation energy are also likely to be important.

The experimental approach outlined in this Letter provides new insight into silicon photodissolution. The identities of the electron-injecting intermediates remain to be established, and it would therefore be interesting to combine the approach outlined in this Letter with *in situ* infrared spectroscopy. Further work on this aspect of the problem is in progress.

¹H. Gerischer and F. Beck, *Z. Phys. Chem.* **24**, 378 (1960).

²R. Memming and G. Schwandt, *Surf. Sci.* **4**, 109 (1966).

³M. Matsamura and S. R. Morrison, *J. Electroanal. Chem.* **144**, 113 (1983).

⁴M. Matsamura and S. R. Morrison, *J. Electroanal. Chem.* **147**, 157 (1983).

⁵H. Gerischer and M. Lubke, *Ber. Bunsenges. Phys. Chem.*

91, 394 (1987).

⁶J. Stumper and H. J. Lewerenz, to be published.

⁷J. Li and L. M. Peter, *J. Electroanal. Chem.* **199**, 1 (1986).

⁸R. Peat and L. M. Peter, *Ber. Bunsenges. Phys. Chem.* **91**, 381 (1987).

⁹R. Peat and L. M. Peter, *J. Electroanal. Chem.* **209**, 307

(1986).

¹⁰H. J. Lewerenz, J. Stumper, and L. M. Peter, to be published.

¹¹E. Yablonovitch, D. L. Allara, C. C. Chang, T. Gmitter, and T. B. Bright, *Phys. Rev. Lett.* **57**, 249 (1986).

¹²L. M. Peter, D. J. Blackwood, and S. Pons, to be published.